

Quantum Chemical Studies on Corrosion Inhibition of 1,3-Thiazine Derivatives for Mild Steel in Acidic Media: DFT Approach

Olofinjana Sikemi, Oyebamiji Abel Kolawole, and Semire Banjo*

Department of Pure and Applied Chemistry, Faculty of Pure and Applied Sciences,
Ladoke Akintola, University of Technology, P.M.B. 4000, Ogbomosho, Oyo State, Nigeria

*Email: bsemire@lautech.edu.ng

ABSTRACT

Quantum chemical calculations via B3LYP/631G(d,p) level were performed on 1,3-Thiazine derivatives used as corrosion inhibitors for mild steel in acidic media. The calculated molecular properties such as the highest occupied molecular orbital energy (E_{HOMO}), Lowest unoccupied molecular orbital (E_{LUMO}), chemical hardness (η), energy band gap (E_g), dipole moment, electronegativity (χ), fraction of electron transfer (ΔN), and global nucleophilicity index (ω) were correlated to the observed corrosion efficiency. The local reactivity indices were analyzed through Fukui functions in order to compare the possible sites for nucleophilic and electrophilic attacks during adsorption of the inhibitors on metal surface. The protonation of the molecular species of the studied thiazines was examined and analyzed.

Keywords: Thiazine derivatives, corrosion inhibition, molecular descriptors, DFT

1.0 INTRODUCTION

Corrosion of mild steel by chemical reactions, which has led to huge economic losses and environmental pollution, has been a major concern in industry. The use of organic compounds containing π -electron either in triple bond or conjugated double bond and heteroatoms such as nitrogen, oxygen, phosphorous, and sulphur as inhibitors has attracted the interest of researchers (Bentiss et al., 2009; Obot et al., 2009; Khaled, 2010; Musa et al., 2010; Mahdavian et al., 2010; Benabdellah et al., 2011; Elayyachy et al., 2011; Zarrok et al., 2011; Doner et al., 2011; Chen et al., 2011; Zhang et al., 2012; Demit et al., 2012; Aahmed et al., 2012; Elyoussfi et al., 2015; Belghiti et al., 2016). Organic compounds are of interest as corrosion inhibitors because they protect/prevent metal from corrosion by formation of film on the metal surface through adsorption. The inhibitory efficiency of compounds is related to the inhibitor adsorption ability, the molecular properties, molecular planarity, and nature of the interaction between the p-orbital of inhibitors with the d-orbital of iron (Sastry, 1998; Bentiss et al., 2009). Therefore, organic compounds that can donate electrons to unoccupied d-orbital of metal surface as well accept free electrons from the metal surface through their anti-bonding orbitals are good corrosion inhibitors. However, nonreactive metals like copper are usually protected by the formation of metal oxide in aqueous medium. In acidic media, the nonreactive metal surface is now unprotected and oxidized to ionic form, thus dissolving readily in an acidic solution (Dortwegt et al., 2001). In the case of copper, there is the oxidization of Cu to Cu^{2+} ions in an acidic medium; therefore, the p-orbital of inhibitors can interact with the d-orbital of copper.

Recently, the inhibiting effect of thiazines—6-(4-methoxyphenyl)-4-phenyl-6H-1,3-

thiazin-2-amine (AT), 6-(4-chlorophenyl)-4-phenyl-6H-1,3-thiazin-2-amine (CBT), and 6-(4-methoxyphenyl)-4-phenyl-6H-1,3-thiazin-2-amine (NBT)—on mild steel corrosion in 1M sulphuric acid (H_2SO_4) was investigated with weight loss, potentiodynamic polarization, and electrochemical impedance spectroscopy (EIS) techniques. The results showed that the inhibitors act as a mixed type, controlling both the anodic and the cathodic reactions with inhibiting action of AT found to be 99 % (Hemapriya et al., 2012). Also, thiazine derivatives have been described as potential organic inhibitors; Larouj et al. (2015) used ethyl 3-hydroxy-8-methyl-4-oxo-6-phenyl-2-(p-toly)-4,6-dihydropyrimido[2,1-b] [1,3]thiazine-7-carboxylate (PT) as a corrosion inhibitor on carbon steel in hydrochloric solution, and the results showed that PT is a good inhibitor with about 95% inhibition efficiency. The inhibiting properties of some organic dyes such as sunset yellow, amaranth, allura red, fast green, and tartrazine were examined on mild steel corrosion in 0.5-M HCl solution. The results showed that the studied dyes are good corrosion inhibitors with enhanced inhibition with tartrazine having the highest inhibition efficiency.

It is now a popular practice to carry out quantum chemical calculations in corrosion inhibition studies due to the pivotal roles played by quantum chemical methods as acceptable tools in elucidating the electronic structure and reactivity of a compound (Kraka et al., 2000). Among other methods, density functional theory (DFT; Parr et al., 1989) is a veritable method in developing new criteria for rationalizing, predicting, and understanding chemical processes. Recently, quantum chemical calculations (especially DFT methods) have been used to study the inhibitory mechanism of organic molecules on a metal surface either as a complementary method to augment the experimental results or as the sole method employed (Rodríguez-Valdez et al., 2004; Blajiev et al., 2004;

Henriquez-Roman et al., 2005; Jamalizadeh et al., 2008; Gece et al., 2010; Semire et al., 2013; Abdulazeez et al., 2016). Therefore, the objective of the present work is to extend the study of the inhibitory properties of 6-(4-methoxyphenyl)-4-phenyl-6H-1,3-thiazin-2-amine (AT), 6-(4-chlorophenyl)-4-phenyl-6H-1,3-thiazin-2-amine (CBT), and

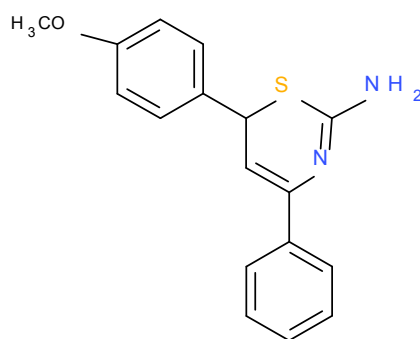
6-(4-methoxyphenyl)-4-phenyl-6H-1,3-thiazin-2-amine (NBT) on mild steel corrosion in 1M sulphuric acid (H_2SO_4 ; Hemapriya et al., 2012) using DFT calculations to look for parameters that characterize the inhibitory property of inhibitors, which will be helpful to gain insight into the mechanism of the corrosion inhibition of the thiazines.

Mol.

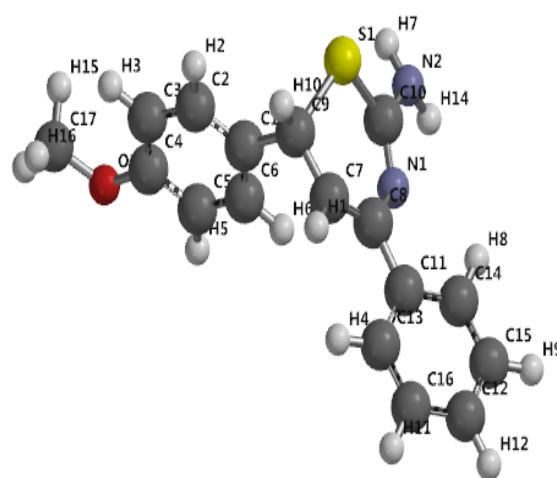
Schematic Structure

Optimized Structure

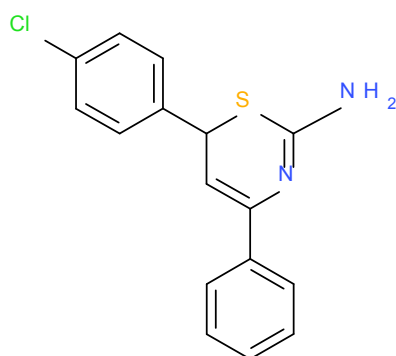
AT



6-(4-methoxyphenyl)-4-phenyl-6H-1,3-thiazin-2-amine



CBT



6-(4-chlorophenyl)-4-phenyl-6H-1,3-thiazin-2-amine

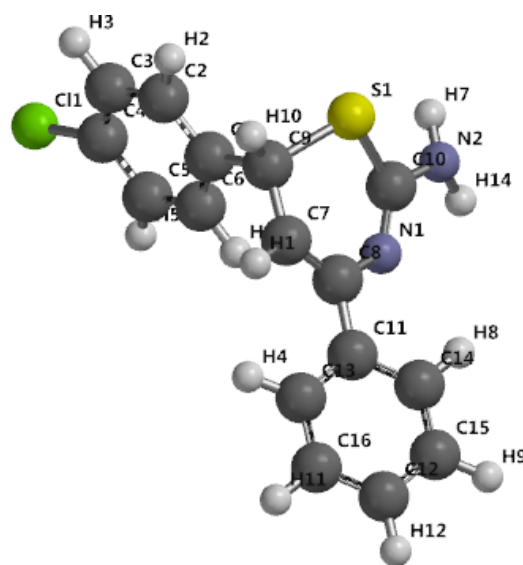


Figure 1. Structures of the examined thiazines.

2.0 COMPUTATIONAL DETAILS

Conformational search was performed on the organic inhibitors using the semi-empirical (AM1) method. For each conformational search, 1000 conformers were examined, and the lowest-energy conformers from this conformational search were taken for further DFT calculations. The lowest-energy conformers of the organic inhibitors were optimized using the density functional theory (DFT) method with Beckes's three-parameter hybrid functional, which employs the Lee, Yang, and Parr correlation functional B3LYP (Becke, 1988; Lee et al., 1988).

Single-point energy calculations were also performed in aqueous medium at the same level of theory on the optimized geometry, obtained in the gas phase. The combination of DFT and 6-31G (d,p) is known to produce a good estimate of molecular properties related to molecular reactivity (Perez et al., 2007; Abdulazeez et al., 2016). The calculated molecular parameters using DFT/6-31G (d,p) include energy of the highest molecular orbital (EHOMO), energy of lowest unoccupied molecular orbital (ELUMO), dipole moment, energy gap electronegativity, hardness, softness, nucleophilicity, chemical potential, and electron affinity. All quantum chemical calculations were performed using Spartan'14 by Wavefunction Inc.

Different chemical theories have been used to explain experimental facts; however, the most promising framework so far is the density functional theory (DFT) of chemical reactivity, also called conceptual DFT. According to Koopman's theorem, this was used for the calculations of global descriptors; softness, electronegativity, chemical potential, and electronegativity are defined in terms of energy of LUMO and HOMO (Rio, 2003) for calculating the global descriptors.

(i) Chemical hardness

$$\eta = \left(\frac{\partial^2 E}{\partial N^2} \right)_{v(r)} = \frac{1}{2} (IP - EA) = \frac{1}{2} (-E_{HOMO} + E_{LUMO})$$

where IP = vertical ionization potential and EA = electron affinity.

$$IP = -E_{HOMO}, EA = -E_{LUMO}$$

(ii) Chemical potential

$$\mu = \left(\frac{\partial E}{\partial N} \right)_{v(r)} = -\frac{1}{2} (IP + EA) \approx \frac{1}{2} (E_{HOMO} + E_{LUMO})$$

(iii) Chemical softness (s): This determines the reactivity of the molecule and it is calculated using the formula

$$(s) = \frac{1}{2\eta}$$

(iv) Electronegativity

$$\chi = \frac{dE}{dN} V(r) = -\chi = -\frac{IP+EA}{2} = \frac{E_{HOMO}+E_{LUMO}}{2}$$

where E is the total energy of the molecule, N is number of electrons and $v(r)$: external potential of the system.

(v) Global electropilicity/ nucleopilicity index,

$$\omega = \frac{\mu^2}{2\eta}$$

(vi) Electron transfer (ΔN): The number of electrons transferred were calculated using

$$\Delta N = \frac{\chi_{Fe} - \chi_{inh}}{2(\eta_{Fe} - \eta_{inh})}$$

where χ_{Fe} and χ_{inh} are the absolute electronegativity of the metal (Fe) and inhibitory molecule, respectively; and η_{Fe} and η_{inh} are the absolute hardness of iron and the inhibitor molecule, respectively (Parr et al., 1978). The value of $\chi_{Fe} = 7.0$ eV and $\eta_{Fe} = 0$ for

the computation of electron transferred.

(vii) Local electropilicity/nucleopilicity index: This is used to determine the reactivity of an individual atom in the molecule as well as its effects in corrosion inhibition for a particular metal. It determines the change in electron density for a nucleophile $F^+_{(r)}$ and $F^-_{(r)}$ as the Funki functions, which can be calculated by the finite differences approximation:

$$F^+_{(r)} = P_{N+1(r)} - P_{N(r)} \quad (\text{for nucleophilic attack})$$

$$F^-_{(r)} = P_{N(r)} - P_{N-1(r)} \quad (\text{for electrophilic attack})$$

where $P_{N+1(r)}$, $P_{N(r)}$, and $P_{N-1(r)}$ are the electronic densities of anionic, neutral, and cationic species, respectively.

3.0 RESULTS AND DISCUSSION

3.1 Molecular Descriptors

The inhibition efficiency of organic inhibitors has been related to the adsorption abilities as well as the molecular properties of the organic inhibitors (Wang et al., 2004). The molecular properties calculated at the B3LYP/6-31G(d,p) level of theory are displayed in Table 1. Also, the energy of the highest occupied molecular orbital (E_{HOMO}) is a measure of the tendency towards the donation of electron by a molecule (Ashry et al., 2006). A high value of E_{HOMO} indicates a high tendency of a molecule to donate electrons to an appropriate acceptor molecule with a low-lying empty molecular orbital. Therefore, an increase in E_{HOMO} values aids adsorption, which will enhance the inhibition efficiency by influencing the transport process through the adsorbed layer. Thus, higher values of E_{HOMO} will lead to an enhanced ability of molecules to donate electrons, which then improves the adsorption ability of the inhibitor on mild steel and therefore brings about better inhibition efficiency. The calculated E_{HOMO} values for AT,

CBT, and NBT are -5.45 , -5.66 , and -5.86 eV, respectively, indicating that AT, with highest E_{HOMO} (-5.45 eV), is the best inhibitor; this agrees with observed inhibition efficiency (Table 1). The E_{LUMO} gives information on the ability of a molecule to accept electrons; therefore, the organic inhibitor with low-lying E_{LUMO} is accepted to have the preferred ability to accept electrons from the d-orbital of metal during the adsorption process. The calculated E_{LUMO} values for AT, CBT, and NBT are -1.01 , -1.26 , and -2.46 eV, respectively, indicating that NBT, with the highest E_{LUMO} (-2.46 eV), will be the best inhibitor to accept from metal with d-electrons; however, this does not correspond to the observed inhibition efficiency.

The binding ability of the inhibitor to the metal surface increases with increase in HOMO and decrease in LUMO energy values because the inhibitors do not only donate electrons to the unoccupied d-orbital of the metal ion but also accept electrons from the d-orbital of the metal leading to the formation of a feedback bond (Breket et al., 2002). Therefore, the energy gap ($\Delta E = E_{\text{LUMO}} - E_{\text{HOMO}}$) is an important parameter that plays a functional role in the reactivity of the inhibitor molecule towards the adsorption on the metallic surface. Lower values of ΔE will support good inhibition efficiency, because the energy to remove an electron from the last occupied orbital will be low (Obot et al., 2009). A molecule with a low energy gap is more polarizable and is generally associated with high chemical activity, low kinetic stability, and high softness value; it is also termed *soft molecule* (Fleming, 1976). Therefore, decrease in value leads to increase in reactivity of the inhibitor towards the metallic surface and enhances adsorption on metal surface, which leads to an increase in %IE of the molecule. However, the trend in calculated ΔE values does not agree with the observed %IE of the molecules (Table 1).

Dipole moment is another important electronic parameter that results from non-

Table 1. Calculated Molecular Parameters at B3LYP/6-31G(d,p)

Parameters	AT	CBT	NBT
E_N (au)	-1240.36667	-1585.43584	-1330.34174
E_{N+1} (au)	-1240.35081	-1585.42985	-1330.36892
E_{N-1} (au)	-1240.11319	-1585.17233	-1330.07043
E_{HOMO} (eV)	-5.45	-5.66	-5.86
E_{LUMO} (eV)	-1.01	-1.26	-2.46
$\Delta E = (E_{LUMO} - E_{HOMO})$	4.44	4.4	3.4
Dipole moment	2.99	1.18	3.96
IP	5.45	5.66	5.86
EA	1.01	1.26	2.46
η (eV)	2.22	2.20	1.70
S (ev)	0.45	0.45	0.59
M	-3.23	-3.46	-4.16
Ω	2.35	2.72	5.09
SE (kJ/mol)	-44.87	-38.45	-43.05
Heteroatom	-0.955	-0.4515	-0.102
ΔN	0.85	0.80	0.84
Inhibition efficiency (%IE)	99.16	96.17	90.24

Note: η = chemical hardness, μ = chemical potential, ω = global nucleophilicity, DM = dipole moment, BG = band gap, SE = solvation energy.

*Heteroatom is the average of electron density on all the heteroatoms present in each molecule, and 'a' = inhibition efficiency was taken from Hemapriya et al., 2012.

uniform distribution of charges on the various atoms in the molecule. The contribution of dipole moment to the adsorption of organic inhibitor to the metal surface has been debated and non-directional (Sastri, 1998; Liu, 2005; Ghazoui et al., 2012). For instance, Eddy et al. (2010) reported that decrease in the value of dipole moment would decrease the inhibition efficiency (Eddy et al., 2011). However, it was also reported by the same in their work that decrease in the value of dipole moment would increase the inhibition efficiency of the inhibitors (Eddy et al., 2011), which is attributed to stronger dipole-dipole interactions of inhibitors and metallic surface. In this study, the ordering of dipole moment values (NBT > AT > CBT) is not consistent with observed % IE.

Moreover, ionization potential (IP), which is a fundamental descriptor of the chemical reactivity of atoms ($IP = -E_{HOMO}$) and molecules, also affects adsorption of inhibitor on metallic surface. A high IP means high stability and chemical inertness while a small IP means high reactivity of the atoms and molecules (Chakraborty et al., 2010). The calculated IP values for AT, CBT, and NBT are 5.45, 5.66, and 5.86 eV, respectively, and this signifies that the AT with the lowest IP has the highest inhibition efficiency, which indicates a better inhibiting efficiency performance in line with the experimental result. Furthermore, chemical hardness (η) and softness are also essential properties in measuring the molecular stability and reactivity. It is important to note that chemical hardness

signifies the resistance towards the distortion or polarization of the electron cloud of the atoms, ions, or molecules under a small perturbation of chemical reaction. A hard molecule has a large energy gap, and a soft molecule has a small energy gap (Obi-Egbedi et al., 2011). The NBT presents the lowest (highest) value of chemical hardness, 1.70 eV (softness, 0.294 eV^{-1}) compared to 2.22 (0.225) and 2.20 eV (0.227 eV^{-1}) for AT and CBT, respectively. The inhibitor with the least value of chemical hardness, that is, the highest softness value, is expected to have the highest inhibition efficiency (Ebenso et al., 2010), which does not correlate to the observed inhibition efficiency.

The global nucleophilicity, ω , shows the ability of the inhibiting molecules to accept electrons. It is a measure of the stabilization in energy after a system accepts additional amount of electron charge from the environment. Therefore, NBT is the strongest electrophile while AT is the strongest nucleophile. For organic inhibitors to be considered suitable, the value of ΔN must be less than 3.6; this means the inhibition efficiency will increase with an increase in the electron-donating ability of the inhibitor to the metallic surface (Lukovit et al., 2001). The ΔN values correlate strongly with experimental inhibition efficiencies; therefore, it can be inferred that inhibitors examined in this study are donors of electrons and the iron surface was the acceptor. Thus, the highest fraction of electrons transferred is associated with the best inhibitors (AT), while the least fraction of electrons transferred is supposed to be associated with the inhibitor that has the least inhibition efficiency (NBT; Udhayakala et al., 2012), but in this study, CBT, which has second highest %IE, shows the lowest ΔN value (Table 1).

Mulliken population analysis is mostly used for the calculation of the charge distribution over the whole molecule, which has been a useful indicator to estimate the adsorption

centers on the inhibitors. The average Mulliken charges on all heteroatoms in each inhibiting molecule (denoted as Heteroatom) are -0.955 , -0.452 , and -0.102 for AT, CBT, and NBT, respectively. It has been established that the more negatively charged a center is, the more it can be adsorbed on the metallic surface (Breket et al., 2012); therefore, higher electron density on heteroatoms of AT facilitates adsorption of the inhibitor on the metallic surface.

3.2 Selection of Suitable Molecular descriptors Through Pearson Matrix

Quantitative structure activity relationships (QSAR) are predictive tools for a preliminary evaluation of the activity of chemical compounds by using computer-aided models. A QSAR is essentially a mathematical equation that is determined from a set of molecules with known activities using computational approaches. The exact form of the relationship between structure and activity can be determined using a variety of statistical methods and computed molecular descriptors, and this equation is then used to predict the activity of new molecules (Rahman et al., 2014). The exact form of the relationship between structure and activity can be determined using a variety of statistical methods as well as calculated molecular descriptors, and this equation is then used to predict the activity of new molecules. In this paper, an attempt is made to correlate the calculated quantum chemical descriptors with the % IE, although a simple/direct relationship is observed with some calculated descriptors and % IE of the inhibitors (Bentiss et al., 2007; Eddy et al., 2009). However, combination of more than one molecular descriptor is usually employed in a composite process like corrosion and inhibition of metal (Obot et al., 2010). The Pearson's correlation matrix is performed on all descriptors by using "MLR" analysis available in SPSS.

The % IE is well correlated with μ ($r = 0.995$), HOMO ($r = 0.980$), LUMO ($r = 0.895$), $\log P$ ($r = 0.807$), and η ($r = 0.955$), while weight ($r = -0.999$) and PSA ($r = -0.876$) are negatively correlated with % IE ($p < 0.05$) at a significant level. Some of the descriptors are well correlated to one another; for instance, the HOMO energy is correlated to μ ($r = 0.956$), LUMO ($r = 0.930$), η ($r = 0.876$), and $\log P$ ($r = 0.672$) and negatively correlated to PSA ($r = -0.761$) and weight ($r = -0.970$) at a $p < 0.05$ level. The Pearson's correlation matrix is used to select the suitable descriptors for MLR analysis, although to develop a good and more valid analysis, the large number of molecules is required. The main objective for developing QSAR model in this work is for careful selection of multiple descriptors, which describes the corrosion inhibition efficiency without multicollinearity. The MLR analysis fits some calculated descriptors and the observed inhibition efficiency of AT, CBT, and NBT very well; the QSAR models are as shown in equations 1, 2, and 3 found to be close to the experimental corrosion inhibition ($R^2 = 1.00$; Table 3).

$$\%IE = 123.418 - 9.334 (\mu) + -0.131 (SE) \quad (1)$$

$$\%IE = 255.263 - 113.760 (Ovality) - 10.457 (Heteroatom) \quad (2)$$

$$\%IE = 123.418 - 9.334 (Volume) + -0.131 (PSA) \quad (3)$$

3.3 Molecular Properties of Protonated AT, CBT, and NBT

Protonation of the studied inhibitor molecules was performed in aqueous medium at

B3LYP/6-31G(d,p) level of theory to deepen the understanding of corrosion inhibitory processes involving the studied molecules, since corrosion of a metal and chemical inhibitory process usually occurs in acidic medium. The protonation sites that lead to low molecular energy are on nitrogen atoms 1 (N1, thiazine nitrogen) and 2 (amino nitrogen) for the examined inhibitors as shown in Figures 2, 3, and 4. The calculations show that more stable geometries are obtained when protonation occurred at N1 (thiazine nitrogen atom), which resulted into about 15-kcal/mol energy difference compared to protonation at N2 (amino nitrogen atom). However, protonation of the neutral molecules (either first and/or second protonation or diprotonation) requires high energy; therefore, it is most probable that the adsorption of these inhibitors on a metallic surface involves neutral molecules.

The protonation of the inhibitors on nitrogen atoms brings about delocalization of the bonds especially C1-C9, C7-C9, and C8-C11. This brings about shortening of bonds when compared to the neutral species as a result of electrons pushing from the two benzene rings into thiazine ring. For instance, the calculated C1-C9, C7-C9, and C8-C11 bond lengths are 1.500, 1.479, and 1.501 Å for ATH^+ (N1); 1.496, 1.482, and 1.502 Å for ATH^+ (N2); and 1.401, 1.463, and 1.417 Å for $AT2H^{++}$, respectively, compared to 1.517, 1.489, and 1.503 Å for AT, respectively (Table 2).

Similar trends are observed for CBT, NBT, and their protonated species. Planarity of molecules is also paramount to the adsorption

Table 3. Experimental and Predicted Inhibition Efficiency (%)

Mol	Exp. Efficiency	Pred. Efficiency (1)	Pred. Efficiency (2)	Pred. Efficiency (3)
AT	99.16	99.15	99.14	99.07
CBT	96.17	96.16	96.17	96.09
NBT	90.24	90.23	90.24	90.14

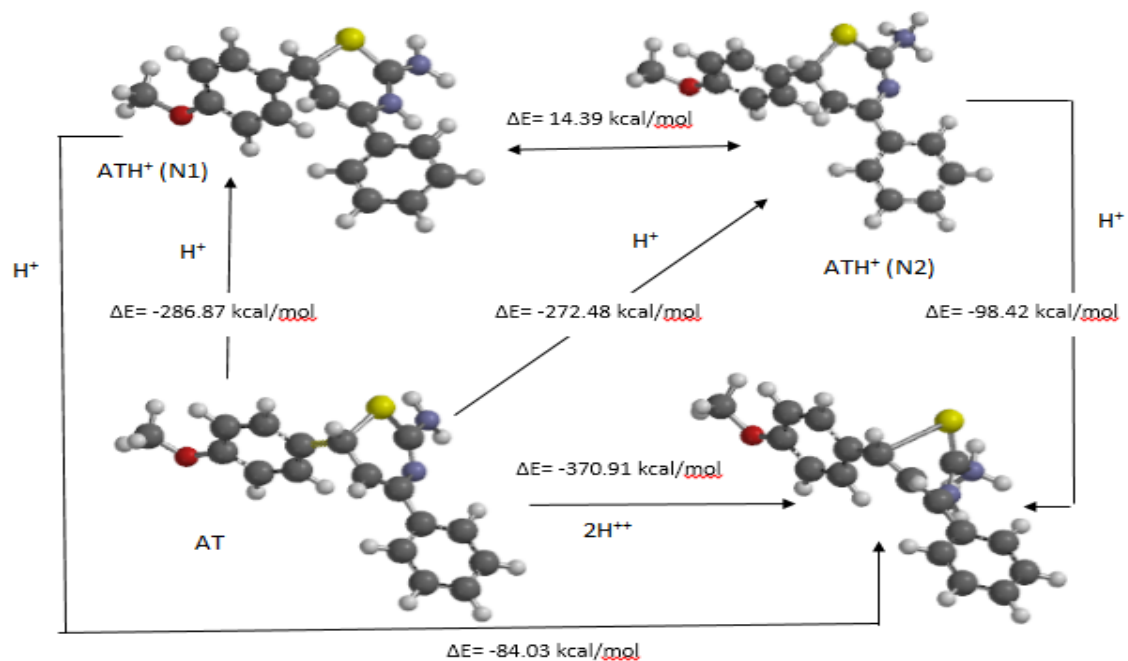


Figure 2. Optimized geometries and relative stability of mono- and diprotonated AT.

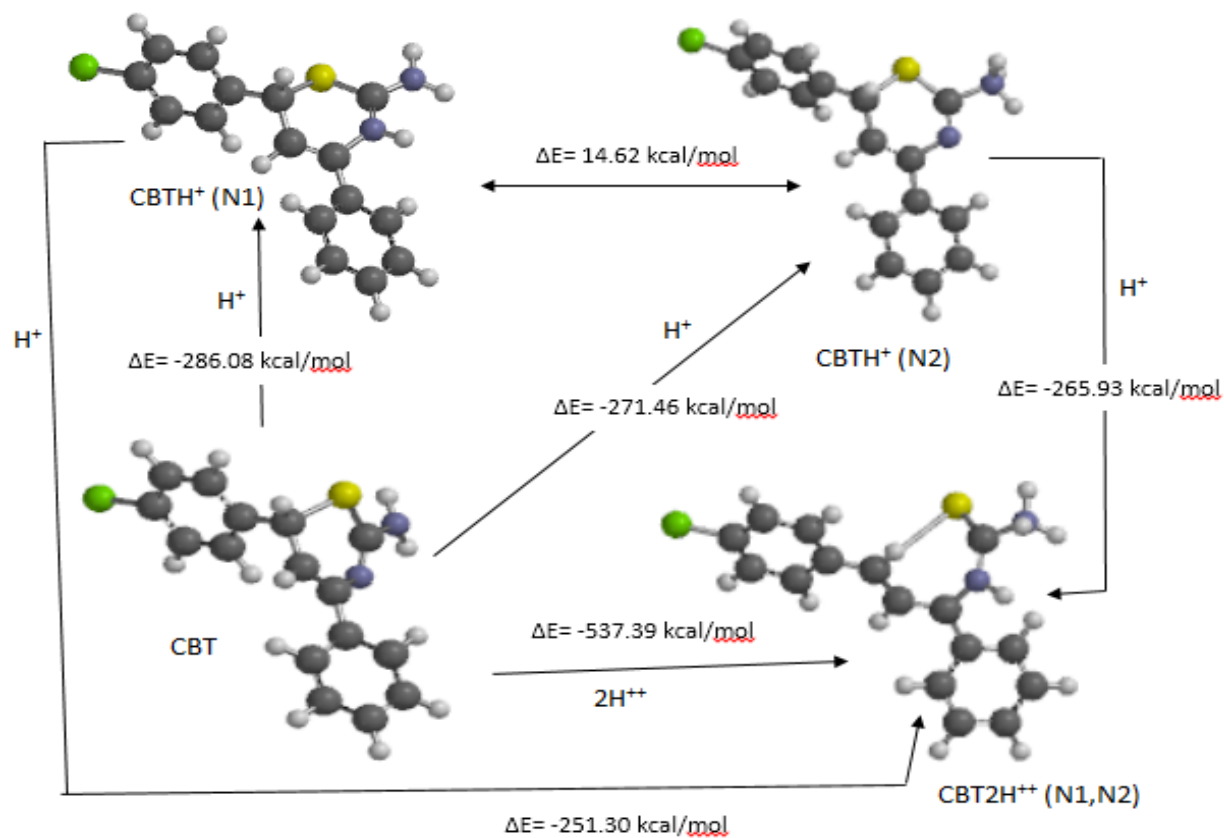


Figure 3. Optimized geometries and relative stability of mono- and diprotonated CBT.

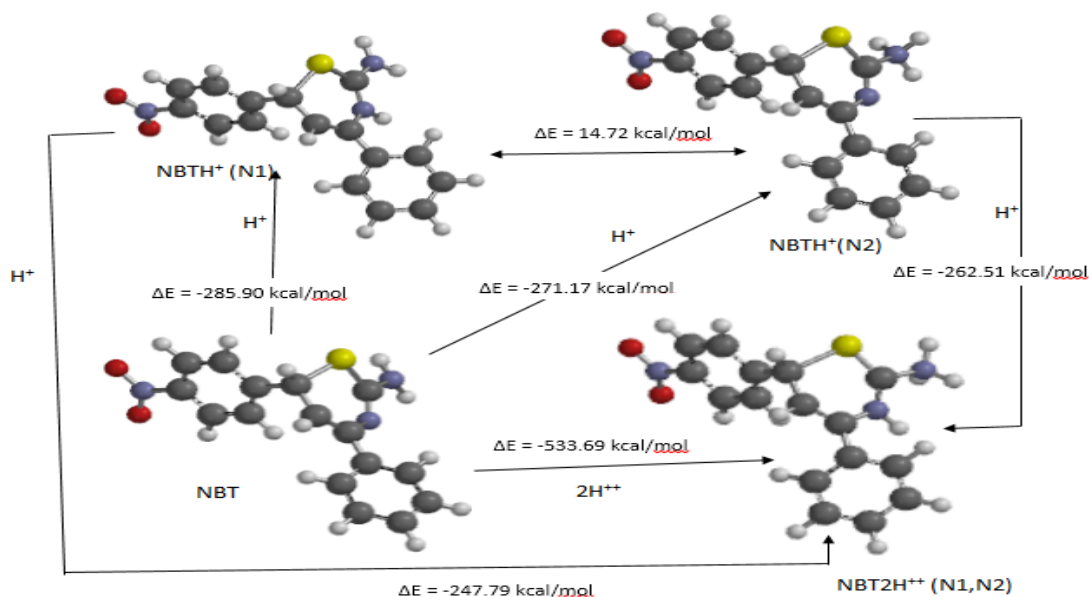


Figure 4. Optimized geometries and relative stability of mono- and diprotonated NBT.

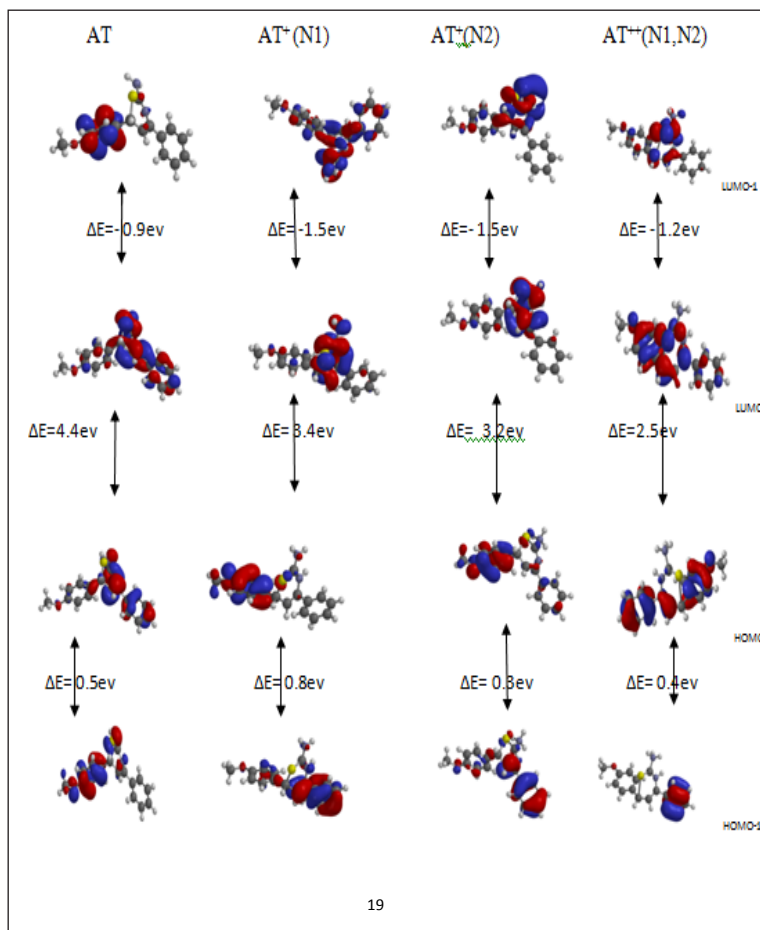
of inhibitor on the metallic surface. However, both neutral and protonated inhibitors are distorted from planarity, although the protonated species are slightly more distorted. For a neutral AT molecule, dihedral angles (C6-C1-C9-C7 and C7-C8-C11-C13) are calculated to be -37.17° and 21.19° ; these are calculated to be -38.31° and 39.95° for ATH^+ (N1), 37.08° and 24.90° for ATH^+ (N2), and 6.86° and 34.37° for AT2H^{++} (N1,N2), respectively, as shown in Table 4. Therefore, it is suggested that the adsorption of these inhibitors on a metallic surface depends less on planarity, but they are rather facilitated by electrostatic attractions and formation of partially weak bonds between the heteroatoms and the metallic surface.

The frontier molecular orbital maps composed of HOMO, HOMO-1, LUMO, and LUMO+1 for the neutral and protonated molecules are shown in Figures 5, 6, and 7 for AT, CBT, and NBT, respectively. The analysis of electronic properties of the protonated species reveals a change in chemical properties such as the electron donating capability of the inhibitors to the metal. The energy gap

of $E_{\text{HOMO}} - E_{\text{HOMO-1}}/E_{\text{LUMO}} - E_{\text{LUMO+1}}$ decreases/increases with an increase in number of protons for protonation. The energy of the HOMO is lower in the protonated species than in the nonprotonated species, which is an indication that protonation decreases the electron donating ability of the inhibitors; however, the energy of the LUMO is lower in the protonated species than in the nonprotonated species indicating that there is an increase in electron accepting ability of the inhibitors from the d-orbital of the metal (Mwadham et al., 2012). A low energy gap coupled with structural stabilities should favour the adsorption of protonated species on a metallic surface. Without any prejudice to the early proposition, it has been argued that at low concentrations and before the equilibrium, more of the protonated species will be adsorbed to the metallic surface. Nevertheless, at high concentrations and toward equilibrium, desorption of the protonated species will be rapid from the metallic surface due to charge repulsion, and molecular distortion of the molecules from planarity thereby facilitates the adsorption of neutral species at equilibrium (Semire et al., 2013).

Table 4. Energies and Selected Geometries of the Neutral and Protonated Species

Inhibitor	HOMO (eV)	LUMO (eV)	ΔE (eV)	Energy (au)	C1-C9 (Å)	C7-C9 (Å)	C8-C11 (Å)	C6C1C9C7/ C7C8C11C13
AT	-5.45	-1.01	4.44	-1240.38378	1.517	1.489	1.503	-37.17/21.19°
ATH ⁺ (N1)	-8.70	-5.30	3.40	-1240.84095	1.500	1.479	1.501	-38.31/39.95°
ATH ⁺ (N2)	-8.70	-5.50	3.20	-1240.81801	1.496	1.482	1.502	-37.08/24.90°
AT2H ⁺⁺ (N1,N2)	-12.40	-9.90	2.50	-1240.97487	1.401	1.463	1.417	6.86/34.37°
CBT	-5.66	-1.26	4.40	-1585.45060	1.520	1.503	1.489	-33.53/-22.79°
CBTH ⁺ (N1)	-9.40	-5.60	3.80	-1585.90651	1.508	1.502	1.477	-44.84/-37.30°
CBTH ⁺ (N2)	-9.10	-5.70	3.40	-1585.88321	1.509	1.505	1.479	-47.35/28.25°
CBT2H ⁺⁺ (N1,N2)	-12.60	-10.3	2.30	-1586.30700	1.410	1.402	1.450	-5.12/-26.57°
NBT	-5.86	-2.46	3.40	-1330.35820	1.522	1.502	1.488	-29.36/23.61°
NBTH ⁺ (N1)	-9.80	-5.80	4.00	-1330.81381	1.515	1.502	1.478	-32.20/37.71°
NBTH ⁺ (N2)	-9.30	-6.00	3.30	-1330.79035	1.513	1.503	1.480	-32.07/24.96°
NBT2H ⁺⁺ (N1,N2)	-12.90	-10.90	2.00	-1331.20870	1.478	1.496	1.473	-31.97/40.59°

**Figure 5.** The frontier molecular orbitals: HOMO, HOMO+1, LUMO, and LUMO-1 of neutral and protonated AT.

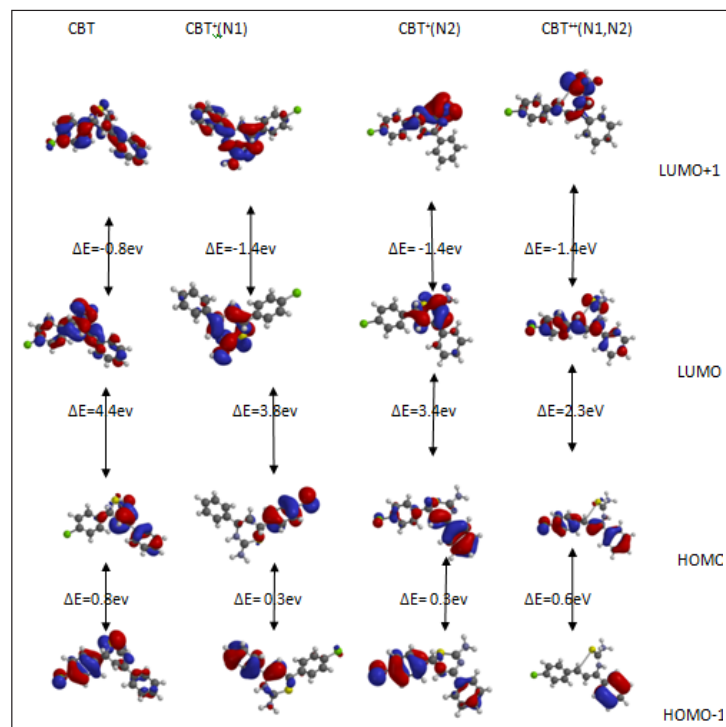


Figure 6. The frontier molecular orbitals: HOMO, HOMO+1, LUMO, and LUMO-1 of neutral and protonated CBT.

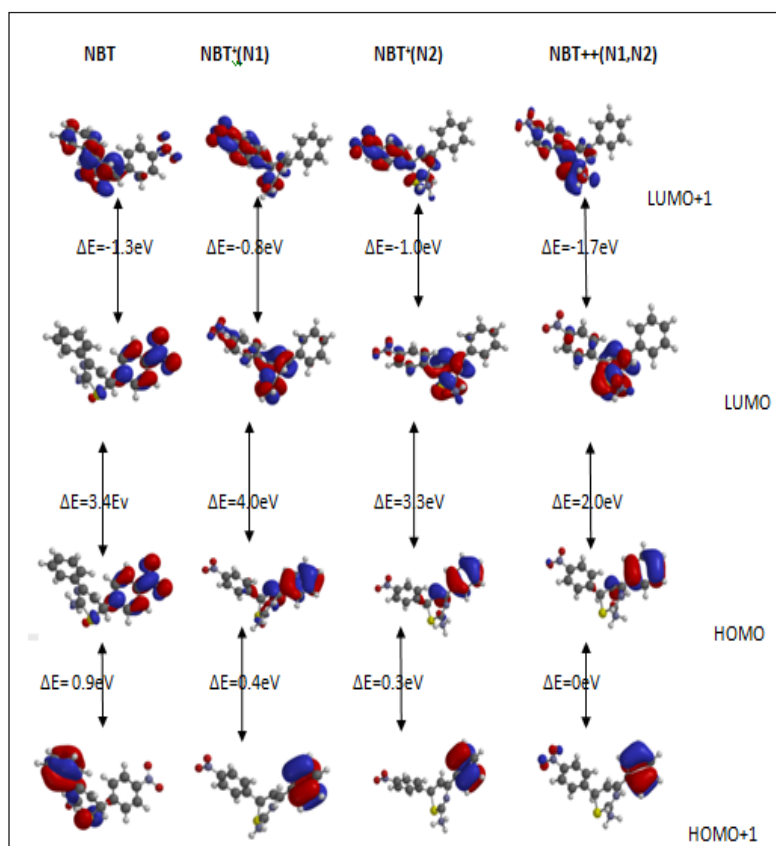


Figure 7. The frontier molecular orbitals: HOMO, HOMO+1, LUMO, and LUMO-1 of neutral and protonated NBT.

3.4 Local Reactivity Descriptors

The use of electron population density analysis to estimate the adsorption centers of inhibitors has been widely reported, and it has been used to calculate charge distribution over the whole skeleton of the molecule (Sahin et al., 2008). Therefore, it is very imperative to consider the situation corresponding to a molecular center that is going to receive a certain amount of charge at some other center as well as a molecular center that is going to donate back a certain amount of charge through the same center or another one (Gomez et al., 2006). There is a general consensus by many authors that the more negatively charged a heteroatom is, the more it can be adsorbed on the metal surface through the donor-acceptor type reaction (Obot et al., 2009). Also, Parr and Yang proposed that a larger value of Fukui function indicates better reactivity than lower values (Parr, 1989); hence, the greater the value of condensed Fukui index, the more reactive is the particular atomic center in the molecule.

The local reactivity of the molecules is usually analyzed by means of the condensed Fukui functions. The condensed Fukui functions allow one to distinguish each part of the molecule on the basis of its distinct chemical behaviour due to the different substituted functional group (Fukui et al., 1952). In order to determine the nucleophilic (f_k^+) and electrophilic (f_k^-) centers of attraction in the molecules, the situation that corresponds to the centers of the molecule that will carry a certain amount of charge is considered. The Fukui indices (f_k^+ and f_k^-) calculated from Mulliken charge population analysis are given in Tables 5 and 6, respectively, for AT, CBT, and NBT inhibitors. The highest value of f_k^- is found on C9 of AT and NBT with 0.027 and 0.036, respectively, whereas for CBT, it is at C5 (0.144), which represents the most probable centers for electrophilic attack. However, the highest value for f_k^+ is found on C9 of each inhibitor with 0.032, 0.030, and 0.022 for AT, CBT, and NBT, respectively. This represents most probable centers for nucleophilic attack in the molecules.

Table 5. Fukui Functions for Electrophilic and Nucleophilic Centers in AT and CBT

AT						CBT					
Atom	$pN_{(r)}$	$pN+1_{(r)}$	$pN-1_{(r)}$	f_k^-	f_k^+	Atom	$pN_{(r)}$	$pN+1_{(r)}$	$pN-1_{(r)}$	f_k^-	f_k^+
S	0.121	-0.034	0.221	-0.100	-0.155	S	0.131	-0.023	0.246	-0.115	-0.154
N ₁	-0.521	-0.540	-0.489	-0.032	-0.019	N ₁	-0.519	-0.539	-0.476	-0.043	-0.02
N ₂	-0.597	-0.618	-0.552	-0.045	-0.021	N ₂	-0.596	-0.617	-0.548	-0.048	-0.021
O ₁	-0.517	-0.530	-0.483	-0.034	-0.013	C ₁	0.161	0.158	0.157	0.004	-0.003
C ₁	0.164	0.169	0.167	-0.003	0.005	C ₂	-0.114	-0.128	-0.111	-0.003	-0.014
C ₂	-0.134	-0.150	-0.126	-0.008	-0.016	C ₃	-0.071	-0.076	-0.060	-0.011	-0.005
C ₃	-0.133	-0.137	-0.112	-0.021	-0.004	C ₄	-0.094	-0.115	-0.092	-0.002	-0.021
C ₄	0.350	0.319	0.369	-0.019	-0.031	C ₅	0.076	-0.089	-0.068	0.144	-0.165
C ₅	-0.120	-0.132	-0.106	-0.014	-0.012	C ₆	-0.111	-0.113	-0.116	0.005	-0.002
C ₆	-0.120	-0.117	-0.120	0.000	0.003	C ₇	-0.134	-0.172	-0.041	-0.093	-0.038

Table 5 continued...

C ₇	-0.129	-0.178	-0.062	-0.067	-0.049	C ₈	0.254	0.222	0.272	-0.018	-0.032
C ₈	0.256	0.222	0.276	-0.020	-0.034	C ₉	-0.363	-0.333	-0.396	0.033	0.030
C ₉	-0.363	-0.331	-0.390	0.027	0.032	C ₁₀	0.302	0.278	0.312	-0.01	-0.024
C ₁₀	0.300	0.270	0.308	-0.008	-0.03	C ₁₁	0.075	0.071	0.082	-0.007	-0.004
C ₁₁	0.074	0.069	0.079	-0.005	-0.005	C ₁₂	-0.081	-0.106	-0.050	-0.031	-0.025
C ₁₂	-0.082	-0.110	-0.054	-0.028	-0.028	C ₁₃	-0.120	-0.134	-0.103	-0.017	-0.014
C ₁₃	-0.120	-0.138	-0.105	-0.015	-0.018	C ₁₄	-0.100	-0.111	-0.074	-0.026	-0.011
C ₁₄	-0.100	-0.113	-0.077	-0.023	-0.013	C ₁₅	-0.092	-0.097	-0.084	-0.008	-0.005
C ₁₅	-0.092	-0.099	-0.085	-0.007	-0.007	C ₁₆	-0.094	-0.096	-0.087	-0.007	-0.002
C ₁₆	-0.095	-0.096	-0.088	-0.007	-0.001	Cl	-0.025	-0.112	0.047	-0.072	-0.087
C ₁₇	-0.079	-0.058	-0.105	0.026	0.021						

Table 6. Fukui Functions for Electrophilic and Nucleophilic Centers in NBT

Atom	pN _(r)	pN+1 _(r)	Pn-1 _(r)	f _k ⁻	f _k ⁺
S	0.139	0.036	0.261	-0.122	-0.103
N ₁	-0.515	-0.533	-0.469	-0.046	-0.018
N ₂	-0.595	-0.611	-0.547	-0.048	-0.016
N ₃	0.385	0.339	0.388	-0.003	-0.046
O ₁	-0.398	-0.520	-0.371	-0.027	-0.122
O ₂	-0.397	-0.518	-0.375	-0.022	-0.121
C ₁	0.174	0.152	0.168	0.006	-0.022
C ₂	-0.127	-0.138	-0.126	-0.001	-0.011
C ₃	-0.089	-0.115	-0.077	-0.012	-0.026
C ₄	0.245	0.234	0.254	-0.009	-0.011
C ₅	-0.095	-0.126	-0.084	-0.011	-0.031
C ₆	-0.125	-0.135	-0.133	-0.008	-0.010
C ₇	-0.138	-0.141	-0.034	-0.104	-0.003
C ₈	0.253	0.241	0.269	-0.016	-0.012
C ₉	-0.366	-0.344	-0.402	0.036	0.022
C ₁₀	0.303	0.301	0.313	-0.010	-0.002
C ₁₁	0.075	0.075	0.084	-0.009	0.000
C ₁₂	-0.081	-0.093	-0.047	-0.034	-0.012
C ₁₃	-0.119	-0.125	-0.102	-0.017	-0.006
C ₁₄	-0.099	-0.105	-0.072	-0.027	-0.006
C ₁₅	-0.092	-0.094	-0.083	-0.009	-0.002
C ₁₆	-0.094	-0.096	-0.086	-0.008	-0.002

4.0 CONCLUSION

The relationships between the inhibition efficiencies of mild steel molecular descriptors/parameters such as E_{HOMO} , E_{LUMO} , energy gap (ΔE), hardness (η), softness (S), chemical potential (μ), electron affinity (EA), the fraction of electron transferred (ΔN), and electrophilicity index (ω) for 3-Thiazine derivatives on mild steel are calculated using quantum chemical method via the B3LYP/6-31G** level of theory. The neutral species of the compounds are most favored to be adsorbed on the metal surface at equilibrium and high concentration than protonated species due to charge repulsion and a higher energy of protonation. However, the QSAR approach used in the study shows a good relationship between the experimental results and the predicted % IE. Therefore, it is observed that AT has a promising ability as a corrosion inhibitor compared to CBT and NBT.

REFERENCES

- Abdulazeez M. O., Oyebamiji A. K., & Semire, B. (2016). DFT and QSAR study of corrosion inhibition on 3,5-di-substituted pyrazole derivatives with heteroatom on position one. *Lebanese Science Journal*, 17(2), 217–232.
- Ahamad, I., Prasad, R., Ebenso, E.E., & Quraishi, M.A. (2012). Electrochemical and quantum chemical study of Albendazole as corrosion inhibitor for mild steel in hydrochloric acid solution. *International Journal of Electrochemical Science*, 7, 3436–3454.
- Ashry, E. L., Nemr, A., Esawy, A. S., Ragab, S. A. (2006). Corrosion inhibitors: Part II: Quantum chemical studies on the corrosion inhibition of steel in acidic medium by some triazole, oxidazole and thiadiazole derivatives. *Electrochimica Acta*, 51, 3957–3968.
- Becke, A. D. (1988). Density-functional thermochemistry. III. The role of exact exchange. *Physical Review A*, 38, 3098–3100.
- Belghiti, M. E., Karzazi, Y., Tighadouini, S., Dafali, A., Jama, C., Warad, I., Hammouti, B., & Radi, S. (2016). New hydrazine derivatives as corrosion for mild steel in phosphoric acid medium. Part B: Theoretical investigation. *Journal of Materials and Environmental Science*, 7(3), 956–967.
- Benabdellah, M., Yahyi, A., Dafali, A., Aouniti, A., Hammouti, B., & Ettouhami, A. (2011). Corrosion inhibition of steel in molar HCl by trphenyltin2-thiophene carboxylate. *Arabian Journal of Chemistry*, 4, 343–347.
- Bentiss, F., Jama, C., Mernari, B., El Attari, H., El Kadi, L., Lebrini, M., Traisnel, M., & Lagrenée, M. (2009). Corrosion control of mild steel using 3,5-bis(4-methoxyphenyl)-4-triazole in normal hydrochloric acid medium. *Corrosion Science*, 51(8), 1628–1635.
- Bentiss, F., Jama, C., Mernari, B., El Attari, H., El Kadi, L., Lebrini, M., Traisnel, M., & Lagrenée, M. (2009). Corrosion control of mild steel using 3, 5-bis (4-methoxyphenyl)-4-amino-1, 2, 4-triazole in normal hydrochloric acid medium. *Corrosion Science*, 51, 1628–1635.
- Bentiss, F., Lebrini, M., Lagrenée, M., Traisnel, M., Elfarouk, A., & Vezin, H. (2007). The influence of some new 2,5-disubstituted 1,3,4-thiadiazoles on the corrosion behaviour of mild steel in 1M HCl solution: AC impedance study and theoretical approach. *Electrochimica Acta*, 52, 6865.
- Blajiev, O., & Hubin, A. (2004). Inhibition of copper corrosion in chloride solutions by amino-mercapto-thiadiazole and methyl-mercapto-thiadiazole: An impedance spectroscopy and a quantum chemical investigation. *Electrochimica Acta* 49, 2761–2770.
- Breket, G., Hur, E., & Ogretir, C. (2002). Quantum chemical studies of some pyridine derivatives as corrosion inhibitor in acidic medium. *Journal of Molecular Structure: THEOCHEM*, 79, 578.
- Chakraborty, T., & Ghosh, D. C. (2010). Computational of the atomic radii through the conjoint action of the effective nuclear charge and the ionization energy. *Molecular Physics*, 108(16), 2081.
- Chen, W., Luo, H. Q., & Li, N.B. (2011). Inhibition effects of 2,5-dimercapto-1,3,4-thiadiazole on the corrosion of mild steel in sulphuric acid solution. *Corrosion Science*, 53, 3356–3365.

- Demet, O.K, Bayol, E., Ali, A. G., & Fatina, K. (2012). The inhibition effect of Azure A on mild steel in 1 M HCl. A complete study: Adsorption, temperature, duration and quantum chemical aspects. *Corrosion Science*, *56*, 143–152.
- Doner, A., Solmaz, R., Özcan, M., & Kardas, G. (2011). Experimental and theoretical studies of thiazoles as corrosion inhibitors for mild steel in sulphuric acid solution. *Corrosion Science*, *53*, 2902–2913.
- Ebenso, E. E., David, I. A., & Eddy, O. (2010). Adsorption and quantum studies on the inhibition potentials of some thiosemicarbazides for the corrosion of mild steel in acidic medium. *International Journal of Molecular Sciences*, *11*, 2473–2498.
- Eddy, N. O., Awe, F. E., Gimba, C. E., Ibisi, N. O., & Ebenso, E. E. (2011). QSAR, experimental and computational chemistry simulation studies on the inhibition potentials of some amino acids for the corrosion of mild steel in 0.1 M HCl. *International Journal of Electrochemical Science*, *6*, 931–957.
- Eddy, N. O., Ibok, U. J., Ebenso, E. E., El-Nemr, A., & El-Sayed El-Ashry, H. (2009). Quantum chemical study of the inhibition of the corrosion of mild steel in H₂SO₄ by some antibiotics. *Journal of Molecular Modeling*, *15*, 1085.
- Elayyachy, M., Hammouti, B., El Idrissi, A., & Aouniti, A. (2011). Adsorption and corrosion inhibition behaviour of C38 steel by one derivative of quinoxaline in 1M HCl. *Portugaliae Electrochimica Acta*, *29*, 57–68.
- Elyoussfi, A., Elmsellem, H., Dafali, A., Cherrak, K., Sebbar, N. K., Zarrouk, A., Essassi, E. M., Aouniti, A., El Mahi, B., & Hammouti, B. (2015). Adsorption and corrosion inhibition of mild steel in 0.5 M H₂SO₄ by a new thiazine derivative 2H-benzo[b][1,4]thiazin-33(4H)-one using experimental and theoretical approaches. *Der Pharma Chemica*, *7*(10), 284–291.
- Fleming, I. (1976). *Frontier orbitals and organic chemical reactions*. 2nd ed. New York: John Wiley and Sons.
- Fukui, K., Yonezawa, T., & Shingu, H. (1952). A molecular orbital theory of reactivity in aromatic hydrocarbons. *Journal of Chemical Physics*, *20*(4), 722.
- Gece, G., & Bilgic, S. (2010). A theoretical study of some hydroxamic acids as corrosion inhibitors for carbon steel. *Corrosion Science*, *52*, 3304–3308.
- Ghazoui, A., Saddik, R., Benchat, N., Guenbour, M., Hammouti, B., Al-Deyab, S. S., & Zarrouk, A. (2012). Comparative study of pyridine and pyrimidine derivatives as corrosion inhibitors of C38 steel in molar HCl. *International Journal of Electrochemical Science*, *7*, 7080–7097.
- Gomez, B., Likhanova, N. V., Dominguez-Aguilar, M. A., Martinez-Palou, R., Vela, A., & Gasquez, J. (2006). Quantum chemical study of the inhibitive properties of 2-pyridyl-azoles. *Journal of Physical Chemistry*, *110*, 8928.
- Hemapriya, V., Parameswari, K., & Bharathy, G. (2012). The inhibition effect of thiazine compounds towards the corrosion of mild steel in sulphuric acid media. *Rasayan Journal of Chemistry*, *5*(4), 468–476.
- Henriquez-Roman, J. H., Padilla-Campos, L., Paez, M. A., Zagal, J. H., Rubio, M. A., Rangel, C. M., Costamagna, J., & Cardenas-Jiron, G. (2005). The influence of aniline and its derivatives on the corrosion behaviour of copper in acid solution: A theoretical approach. *Journal of Molecular Structure: THEOCHEM*, *757*, 1–7.
- Jamalizadeh, E., Jafari, A. H., & Hosseini, S. M. A. (2008). Semi-empirical and ab initio quantum chemical characterisation of pyridine derivatives as HCl inhibitors of aluminium surface. *Journal of Molecular Structure: THEOCHEM*, *870*, 23–30.
- Khaled, K. F. (2010). A study of the inhibition of iron corrosion in HCl solutions by some amino acids. *Corrosion Science*, *52*, 3225–3234.
- Kraka, E., & Cremer, D. (2000). Computer design of anticancer drugs. *Journal of the American Chemical Society*, *122*, 8245–8264.
- Larouj, M., Lgaz, H., Serrar, H., Zarrok, H., Bourazmi, H., Zarrouk, A., Elmidaoui, A., Guenbour, A., Boukhris, S., & Oudda, H. (2015). Adsorption properties and inhibition of carbon steel corrosion in hydrochloric acid solution by ethyl3-hydroxyl-8-methyl-4-oxo-6-phenyl-2-(p-toyl)-4,6-duhydropyrimido[2.1-b] [thiazine-7-carboxylate. *Journal of Materials and Environmental Science*, *6*(11), 3251–3267.
- Lee, C. T., Yang, W. T., & Parr, R. G. (1988). Development of the Colle–Salvetti correlation-

- energy formula into a functional of the electron density. *Physical Review B*, *37*, 785–589.
- Liu, S. (2005). Dynamic behaviour of chemical reactivity indices in density function theory: A Born–Oppenheimer quantum molecular dynamics study. *Journal of Chemical Sciences*, *117*, 477–483.
- Lukovit, I., Kalman, E., & Zucchi, F. (2001). Corrosion inhibitors—correlation between electronic structure and efficiency. *Corrosion Science*, *57*(1), 3–8.
- Mahdavian, M., & Ashhari, S. (2010). Corrosion inhibition performance of 2-mercatobenzimidazole compounds for protection of mild steel in hydrochloric acid solution. *Electrochimica Acta*, *55*, 1720–1724.
- Musa, A. Y., Kadhun, A. A. H., Mohamad, A. B., & Takriff, M. S. (2010). On the inhibition of mild steel corrosion by 4-amino-5-phenyl-4H-1,2,4-triazole-3-thiol. *Corrosion Science*, *52*, 3331–3340.
- Mwadham, M., Kabanda, M., Lutendo, C.M., & Eno, E.E. (2012). Theoretical studies on phenazin and related compounds as corrosion inhibitors for mild steel in sulphuric acid medium. *International Journal of Electrochemical Science*, *7*, 7179–7205.
- Obi-Egbedi, N. O., Obot, I. B., El-Khaiary, M. I., Umoren, S. A., & Ebenso, E. E. (2011). Computational simulation and statistical analysis on the relationship between corrosion inhibition efficiency and molecular structure of some phenanthroline derivatives on mild steel surface. *International Journal of Electrochemical Science*, *6*, 5649–5675.
- Obot, I. B., & Obi-Egbedi, N. O. (2010). Theoretical study of benzimidazole and its derivatives and their potential activity as corrosion inhibitors. *Corrosion Science*, *52*, 657–660.
- Obot, I. B., Obi-Egbedi, N. O., & Umeren, S. A. (2009). Adsorption characteristics and corrosion inhibitive properties of clotrimazole for aluminium corrosion in hydrochloric acid. *International Journal of Electrochemical Science*, *4*(6), 863–877.
- Parr, R. G., & Yang, W. (1989). *Density functional theory of atoms and molecules*. New York: Oxford University Press.
- Parr, R. G., Donnelly, R. A., & Levy, M. (1978). Amino acid compounds as corrosion inhibition for lead in 0.3 MHCL solution. *Journal of Chemical Physics*, *68*, 3801–3807.
- Perez, A., Luque, F. J., & Orozco, M. (2007). Dynamics of B-DNA on the microsecond time scale. *Journal of the American Chemical Society*, *129*, 14739–14745.
- Rahman, B., Kawano, S., Yunoki-Esaki, K., Anzai, T., & Endo, T. (2014). NMR analyses on the interactions of the yeast Tim50 C-terminal region with the presequence and Tim50 core domain. *FEBS Letters*, *588*(5), 678–684.
- Rodríguez-Valdez, L. M., Martínez-Villafane, A., & Glossman-Mitnik, D. (2004). CHIH-DFT determination of the molecular structure, infrared and ultraviolet spectra of potentially organic corrosion inhibitors. *Journal of Molecular Structure: THEOCHEM*, *681*, 83–88.
- Sahin, M. G. G., Karci, E., & Bilgic, S. (2008). Experimental and theoretical study of the effect of some heterocyclic compounds on the corrosion of low carbon steel in 3.5% NaCl medium. *Journal of Applied Electrochemistry*, *38*(6), 809–815.
- Sastri, V. S. (1998). *Corrosion inhibitors: Principles and applications*. Chichester, England: Wiley.
- Semire, B., & Odunola, A. O. (2013). Density functional theory of the efficiencies of 2-phenylimidazo[1,2-a]pyridine and 2-(m-methoxyphenyl)imidazo[1,2-a]pyrimidine as corrosion inhibitors for mild steel. *Bulgarian Journal of Chemical Education*, *22*(6), 893–906.
- Geerlings, T. H., Faber, A. W., Bister, M. D., Vos, J. C., & Raué, H. A. (2003). Rio2p, an evolutionarily conserved, low abundant protein kinase essential for processing of 20 S pre-rRNA in *saccharomyces cerevisiae*. (2003). *Journal of Biological Chemistry*, *278*(25), 22537–22545.
- Udhayakala, P., Rajendiran, T. V., & Gunasekaran, S. (2012). Quantum chemical studies on the efficiencies of vinyl imidazole derivatives as corrosion inhibitors for mild steel. *Journal of Advanced Scientific Research*, *3*(2), 71–77.
- Wang, H. L., Liu, R. B., & Xin, J. (2004). Inhibiting effects of some mercapto-triazole derivatives on the corrosion of mild steel in 0.1 M HCl medium. *Corrosion Science*, *46*(10), 2455–2466.
- Zarrok, H., Saddik, R., Oudda, H., Hammouti, B., El Midaoui, A., Zarrouk, A., Benchat, N., & Ebn

- Touhami, M. (2011). 5-(2-chlorobenzyl)-2,6-dimethylpyridazin-3-one: an efficient inhibitor of C38 steel corrosion in hydrochloric acid. *Der Pharma Chemica*, *3*, 272–282.
- Zhang, F., Tang, Y., Cao, Z., Jing, W., Wu, Z., & Chen, Y. (2012). Performance and theoretical study on corrosion inhibition of 2-(4-pyridyl)-benzimidazole for mild steel in hydrochloric acid. *Corrosion Science*, *61*, 1–9.
- Dortwegt, R., & Maughan, E.V. (2001). The chemistry of copper in water and related studies planned at the advanced photon source. *Proceedings of the 2001 Particle Accelerator Conference, PAC 2001*. Chicago, pp 1456-1458.

